Measurements and predictions of the $6s6p\ ^{1,3}P_1$ lifetimes in the Hg isoelectronic sequence

L. J. Curtis,* R. E. Irving, and M. Henderson
Department of Physics and Astronomy, University of Toledo, Toledo, Ohio 43606

R. Matulioniene and C. Froese Fischer
Department of Computer Science, Vanderbilt University, Nashville, Tennessee 37235

E. H. Pinnington
Physics Department, University of Alberta, Edmonton Alberta, Canada T6G 2J1
(Received 12 September 2000; published 7 March 2001)

Experimental and theoretical values for the lifetimes of the $6s6p\ ^1P_1$ and $^3P_1$ levels in the Hg isoelectronic sequence are examined in the context of a data-based isoelectronic systematization. New beam-foil measurements for lifetimes in Pb III and Bi IV are reported and included in a critical evaluation of the available database. These results are combined with *ab initio* theoretical calculations and linearizing parametrizations to make predictive extrapolations for ions with $84 \leqslant Z \leqslant 92$.

DOI: 10.1103/PhysRevA.63.042502 PACS number(s): 32.70.Cs, 32.30.Jc

I. INTRODUCTION

Methods that have recently been used to predictively systematize experimental measurements and theoretical calculations for the lowest resonance and intercombination line strengths in the Be [1,2], Sn [3], and Cd [4] isoelectronic sequences are extended to study the Hg sequence. New lifetime measurements are reported, together with a critical evaluation of the existing database, and new multiconfiguration Dirac-Hartree-Fock (MCDHF) *ab initio* calculations are performed. These results are combined to make extrapolative predictions using sensitive linearizing semiempirical methods.

The usefulness of this study for the Hg sequence can be elucidated by a comparison with the homologous Cd sequence. For the Cd sequence, the 48-electron system is sufficiently complex to make its theoretical specification challenging, yet the fact that it begins in the midrange of Z permits it to be followed isoelectronically through many stages of ionization before reaching the high Z limitations on nuclear stability. In contrast, for the Hg sequence the 80-electron system is substantially more complex, and only the first four members are radioactively stable. However, while it is more difficult to measure the atomic structure properties of the radioactive members, their atomic properties are no less significant in, e.g., modeling calculations of radiation transfer in fusion plasmas. Thus, the use of semiempirical methods to accurately extrapolate measurements for Hg I, Tl II, Pb III, and Bi IV through Hg-like uranium and the transuranium ions is highly desirable.

For the Cd sequence, plunging levels from the unfilled $4f$ subshell perturb the $5s5p$ levels above $Z=60$ and eventually replace $5s^2$ as the ground state. In the Hg sequence, our calculations indicate that the $6s6p$ and $6s^2$ levels remain below the plunging levels from the $5f$ and $5g$ subshells for all ions through uranium. Thus these resonance and intercombination transitions can be expected to dominate the radiative transfer among any of the ions in this sequence whenever they exist in a hot plasma environment.

In the study presented here, new beam-foil measurements for the intercombination transition lifetimes for Pb III and Bi IV are reported, together with a critical evaluation of the available database of lifetime measurements. In addition, MCDHF calculations [5] of energy levels and line strengths are reported that include the effects of core-valence correlation. Both the experimental and theoretical results are then systematized using a semiempirical linearization that accurately isoelectronically smooths and extrapolates the results to high Z. The formulation builds on earlier studies of this sequence [6,7], incorporating refinements [2,3] recently made that substantially improve the systematization.

II. SEMIEMPIRICAL FORMULATION

In the semiempirical formulation used here, the $ns^2\ ^1S_0 - nsnp\ ^1P_1$ resonance transition and the $ns^2\ ^1S_0 - nsnp\ ^3P_1$ intercombination transition are treated jointly by removing the effects of intermediate coupling through the use of a singlet-triplet mixing angle θ [3,8] that is empirically evaluated from energy-level data.

In the nonrelativistic approximation, these two transitions are described by the same radial dipole transition element. In the corresponding relativistic formulation, each of these radial transition elements becomes a separate admixture of two jj radial matrix elements.

It has been shown earlier [2] that both the LS singlet-triplet mixing in the angular wave function and the jj mixing in the radial wave function can be simultaneously taken into account for s^2-sp transitions through the specification of a second effective mixing angle, denoted here by ξ. Theoretical calculations have shown [2] that the radial mixing angle ξ is usually quite small unless there are strong cancellation effects. Moreover, in cases in which ξ becomes significant, it usually affects only ions near the neutral end of the sequence where θ is smallest. Until now, this correction has been ap-

*Electronic address: ljc@physics.utoledo.edu

plied [2] only to the Be $2s^2-2s2p$ sequence, where the LS singlet-triplet mixing of the neutral ion is so small that the jj radial mixing becomes non-negligible. For the Mg, Zn, and Cd sequences, the LS singlet-triplet mixing angle is large compared to the jj radial mixing angle for all ions in the sequence. However, for the Hg sequence our calculations show that these corrections are significant for the neutral and singly ionized members of the sequence.

For the unbranched $ns^2\,{}^1S_0-nsnp\,{}^1P_1$ resonance and $ns^2\,{}^1S_0-nsnp\,{}^3P_1$ intercombination transitions, the line strengths S(res) and S(int) can be deduced from the lifetimes τ and the transition wavelengths λ using

$$S=[\lambda(\text{Å})/1265.38]^3\ \ 3/\tau(\text{ns}). \tag{1}$$

In the absence of significant configuration interaction, both the energy levels and the line strengths can be characterized by the singlet-triplet mixing angle amplitudes that couple the $J=1$ levels. It has been shown [8] that these can be modeled using a one-to-one mapping of the three independent separations among the $nsnp\,{}^3P_0$, ${}^3P_1$, ${}^3P_2$, and ${}^1P_1$ experimental energy levels onto a set of three effective Slater parameters G_1,μ_1,μ_2 (corresponding to the electron-electron exchange and the diagonal and off-diagonal magnetic interactions). It has been shown [4,3] that the intermediate coupling can be parametrized in terms of a singlet-triplet mixing angle θ prescribed from the energy-level measurements as

$$\cot 2\,\theta=(4G_1+\mu_1)/\sqrt{8}\mu_2. \tag{2}$$

It has also been shown [2] that the effects of differences between the $\{j,j'\}=\{1/2,3/2\}$ and $\{1/2,1/2\}$ relativistic radial transition matrices R_{13} and R_{11} can be incorporated into the characterization through a similar type of mixing angle ξ which, if small, can be prescribed through *ab initio* calculations along an isoelectronic sequence using the relationship [2]

$$\tan\xi=\sqrt{2}(R_{13}-R_{11})/(2R_{13}+R_{11}). \tag{3}$$

These values for θ and ξ can be used to further convert measured lifetime data to the reduced line strengths S_r(res) and S_r(int) [2],

$$S_r(\text{res})\equiv S(\text{res})/\cos^2(\theta-\xi), \tag{4}$$

$$S_r(\text{int})\equiv S(\text{int})/\sin^2(\theta-\xi). \tag{5}$$

These quantities are proportional to the squared radial transition matrices (the weighted sum $2R_{13}^2+R_{11}^2$ for the relativistic formulation). It has been observed that line strengths and mixing angles can often be represented by fitting functions of the form [4]

$$Z^2S_r\cong S_H[1+B/(Z-C_1)], \tag{6}$$

$$\cot 2\,\theta\cong D+E/(Z-C_2) \tag{7}$$

as is illustrated in Figs. 1 and 2. Similarly, the radial transition element ratios were found here to be well represented by

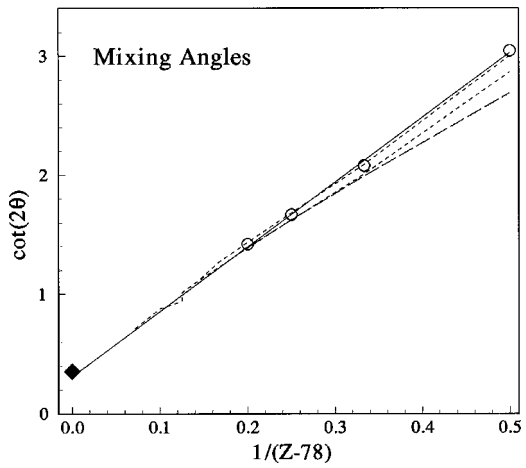

FIG. 1. Isoelectronic plot of $\cot 2\theta$ vs $1/(Z-78)$. The symbols (O) denote the values obtained from the measured data, and the solid line represents a fit of these values to Eq. (7). The short-dashed lines trace the MCDHF values obtained from the ratios of these two amplitudes in each of the two $J=1$ CSF's. The symbol ($\diamond$) is the high-Z asymptotic value 0.353 55 . . . . The long-dashed line traces the corrected value $\cot(2\theta-2\xi)$.

$$R_{13}/R_{11}\cong f+g/(Z-C_3)^p. \tag{8}$$

Here Z is the nuclear charge and B,C_i,D,E,f,g,p are least-squares adjusted fitting constants. S_H could also be evaluated as a fitting parameter, but it has been observed [9] that for very large Z this quantity tends to approach the hydrogenic limit

$$S_H\rightarrow 9n^2(n^2-1)/2. \tag{9}$$

For $n=6$, this yields $S_H=5670$.

III. THEORETICAL CALCULATIONS

Ab initio theoretical calculations were performed to test the persistence to higher Z of the regularities exhibited by the empirical data. With increasing ionicity, it is expected that

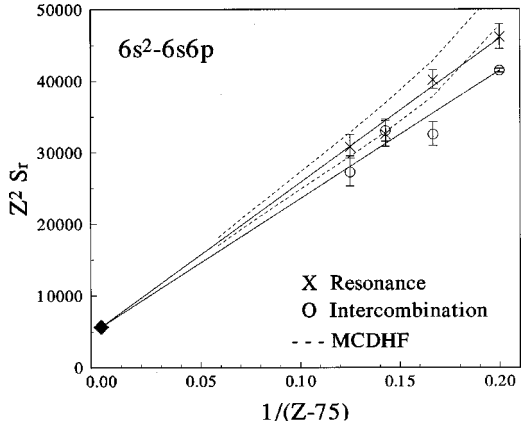

FIG. 2. Isoelectronic plot of the Z^2S_r vs $1/(Z-75)$ for the lowest resonance (X) and intercombination (O) lines. The symbol ($\diamond$) represents the asymptotic value 5670 and the solid lines represent fits to Eq. (6) reported here.

the system will be increasingly influenced by configuration interaction and relativistic effects. MCDHF calculations introduce both additional configurations and the possibility of a significant dependence upon J of the radial transition elements, and can test whether such a system can be characterized at higher Z by the effective mixing angles and reduced line strengths defined here. However, since the MCDHF code treats contributions important at very high Z (e.g., the Breit interaction and *qed* corrections) only perturbatively, there are also limitations to the validity of the theory.

A number of earlier theoretical studies of this sequence have been made. Some have involved specific ions in the sequence [10–13]. Others have utilized a model potential that requires measured spectroscopic data for the evaluation of parameters [14,15], and are not applicable to the entire isoelectronic sequence. One calculation using the multiconfiguration relativistic random-phase approximation [16] studied the entire sequence, but neglected core polarization effects and thus yielded poor agreement [17] with experiment.

The multiconfiguration expansion used here was designed to qualitatively capture both valence and core-valence correlation ($V+CV$) effects. For the even-parity states, the expansion was obtained by single and double excitations of the electrons from the reference set $\{5d^{10}6s^2,\ 5d^{10}6p^2,\ 5d^{10}6d^2 J=0\}$ to an active set of orbitals $\{6s,\ 6p,\ 6d,\ s,\ p,\ d,\ f,\ g\}$, with the constraint of creating at most one hole in the $4d$ subshell. The expansion for the odd-parity states was generated in a similar manner, starting with the reference set $\{5d^{10}6s6p,\ 5d^{10}6p6d\ J=0,1,2\}$, and using the same active set of orbitals as in the case of the even-parity states. The resulting multiconfiguration expansion contained 733 even-parity relativistic configuration state functions (CSF's) of total angular momentum $J=0$, and 5557 odd-parity CSF's with $J=0,1,2$.

The radial orbitals were generated using the optimal level (OL) model. The even-parity level selected for targeting had $6s^2$ as its dominant eigenvector component. The odd-parity states were treated using the extended optimal level model (EOL): four levels (one $J=0$, two $J=1$, and one $J=2$) were targeted under the requirement that the dominant eigenvector component of each selected level be the (nonrelativistic) CSF $6s6p$. The sets of radial orbitals describing the even-parity and the odd-parity states were optimized independently. The radial orbitals were determined in stages, gradually increasing the set of active orbitals. All the core orbitals $(1s\cdots5d)$ were generated by simultaneous optimization in a valence-correlation calculation that included the even-parity $J=0$ levels of $\{6s^2,\ 6p^2,\ 6d^2\}$ and the odd-parity $J=0,1,2$ levels of $\{6s6p,\ 6p6d\}$. The $6s$, $6p$, and $6d$ orbitals were determined variationally in a $V+CV$ calculation with the active orbital set $\{6s,\ 6p,\ 6d\}$, using the core orbitals from the previous calculation. In these two initial stages of the calculation, the levels were assigned statistical weights in the energy functional. In the next stage, the correlation orbitals $\{s,p,d\}$ were added to the active set. The rest of the radial orbitals were taken from the previous calculation, and kept frozen in the variational procedure to determine the correlation orbitals $\{s,p,d\}$. Lastly, $\{f,g\}$ were added in a similar manner. In the two final stages, the levels were assigned equal weights in the energy functional.

IV. NEW MEASUREMENTS FOR THE $^3P_1$ LEVELS IN PB III AND BI IV

The empirical linearity of the plot of Z^2S_r vs $1/(Z-C_1)$ is well established for the resonance transitions, but for the intercombination transitions near the neutral end of the sequence, the small mixing and long lifetimes make these determinations more uncertain.

Attempts were made in a 1996 study of Tl II [7] to verify the linear trends for the intercombination line strengths. Based on a linear extrapolation of the high-Z asymptote and the reduced line strengths obtained from the earlier lifetime measurements made at the University of Alberta [18–20] for Bi IV and Pb III, a prediction for the Tl II intercombination lifetime of 31 ± 2 ns was obtained. A measurement of this quantity was made at the Toledo Heavy Ion Accelerator (THIA) laboratory, which yielded 39 ± 3 ns. Since the discrepancy is more than two standard deviations (uncertainties combined in quadrature), this motivated further study to determine whether it indicates a breakdown of the semiempirical linearity, systematic experimental uncertainties, or simple statistical scatter in a normal sample distribution.

In an attempt to resolve this discrepancy, new beam-foil measurements of the Pb III and Bi IV intercombination lines were undertaken in the THIA laboratory. The values (obtained using the methods described in Ref. [7]) were consistent with the Alberta results [19,20], but in both cases the values were one standard deviation on the long lifetime side. Since the Alberta and THIA measurements were obtained using different accelerators, beam energies, foil thickness, etc., each approach had different advantages and disadvantages. Therefore, the two laboratories undertook a joint restudy to replace the symmetric quoted uncertainties with firm upper and lower limits. The goal was to determine whether the two sets of measurements bracket the correct result or if one of the measurements is to be preferred.

On the basis of this reanalysis, it was possible to effectively rule out systematic errors due to factors such as foil thickness, energy loss in the foil, divergence of the ion beam, or straggling. It was also possible to utilize a comparison of results obtained by the correlated ''analysis of decay curve'' (ANDC) [21] method with simple curve-fitting results to set upper limits on the lifetimes. For the intercombination transitions in both ions, the nature of the cascade decay curves incorporated into the ANDC analysis had properties that reduced the extracted lifetime from an overestimate obtained by simple multiexponential fitting. Thus the simple fitted value represents a firm upper limit, and simulations and tests were undertaken to ascertain whether uncertainties in the measured cascade could lead to uncertainties on the short lifetime side.

For the singlet decays, it was confirmed that the data were of consistently good quality, and that the lifetime values extracted were not significantly dependent on the method of

TABLE I. Calculated and observed energy levels (in cm^{-1}).

	$^3P_0$		$^3P_1$		$^3P_2$		$^1P_1$	
Z	MCDHF	Obs	MCDHF	Obs	MCDHF	Obs	MCDHF	Obs
80	37 935	37 645.080	39 709	39 412.300	44 337	44 042.977	55 250	54 068.781
81	49 669	49 451	52 595	52 393	61 841	61 725	76 107	75 660
82	60 653	60 397.	64 609	64 391.	79 024	78 984.6	95 535	95 340.1
83	71 188	70 963	76 101	75 926	96 333	96 423	114 590	114 602
84	81 421		87 235		113 973		133 698	
85	91 427		98 100		132 064		153 083	
86	101 207		108 704		150 652		172 847	
87	110 874		119 167		169 897		193 182	
88	120 460		129 526		189 876		214 186	
89	129 913		139 732		210 586		235 869	
90	139 281		149 838		232 126		258 338	
91	148 592		159 873		254 576		281 682	
92	157 863		169 856		278 008		305 976	

analysis (whether free multiexponential fitting, constrained multiexponential fitting, or ANDC reduction). Thus, most of the restudy concerned attempts at improving the precision of the triplet lifetime values.

Based on this careful reexamination, the best results for the $6s6p\ ^3P_1$ lifetimes, as deduced from the THIA measurements, are 17 ± 2 ns for Pb III and 9.2 ± 10 ns for Pb IV. For the Alberta measurement of Pb III, the value of 14.8 ns remains valid, but the uncertainty is skewed slightly toward longer lifetime. Extensive reanalysis indicates that, if symmetric uncertainties are quoted, a value 15.2 ± 1.0 provides a better lower limit. For the Alberta measurement of Bi IV, the value 8.0 ns is a firm lower limit, and the uncertainties should be increased slightly, to 9.0 ± 1. We have combined all of these measurements to obtain recommended values for the $6s6p\ ^3P_1$ lifetimes τ (Pb III)$=15.2\pm0.7$ ns and τ (Bi IV)$=9.1\pm0.7$ ns.

V. RESULTS

A. Energy levels and mixing angles

The available base of measured energy level data [22] is presented in Table I, together with the MCDHF predictions obtained from the calculations reported here. The small discrepancies between the theoretical and observed energy levels reflect the uncertainties in the calculation. To within these tolerences, the magnitudes and signs of these differences are sensitive to the configurations included and to the core polarizability through their influence on the depth of the binding energy of the ground state and the relative positions of the singlet and triplet systems.

The measured base of energy-level data was used to specify the LS mixing angles θ using Eq. (2). These mixing angles were then isoelectronically parametrized using the fitting function of Eq. (7) (with $p=1.6$ and $C_2=78$ deduced from a log-log exposition). This yielded $D=0.3096$ (slightly less than the jj asymptotic limit $1/\sqrt{8}=0.353\,55\ldots$) and $E=5.437$. A plot of $\cot 2\theta$ vs $1/(Z-78)$ is presented in Fig. 1.

The corresponding mixing angles were also computed from the CSF amplitudes obtained from the MCDHF calculation. Since this was a multiconfiguration calculation, there were more than two amplitudes to consider, but effective mixing angles could be obtained by defining $\tan\theta_1$ to be the ratio between the $6s6p\ ^3P_1$ and $6s6p\ ^1P_1$ amplitudes for the higher (nominal singlet) $J=1$ CSF, and defining $\cot\theta_3$ to be the same ratio for the lower (nominal triplet) $J=1$ CSF. The deviation of the quantity $\sin^2\theta_1+\cos^2\theta_3$ from unity then becomes a measure of the ability of the single configuration model to include the effects of configuration interaction through the use of effective mixing angles. These MCDHF results are shown as short-dashed curves in Fig. 1.

A comparison of the quantity R_{13}/R_{11} for the Be, Mg, Zn, Cd, and Hg sequences is shown in Table II. These calculations used the MCDHF program, but made the simplest baseline computation that did not include correlation. These results clearly demonstrate that the correction can be neglected for the homologous systems through the Cd sequence, but become significant for the Hg sequence. The values of R_{13}/R_{11} for the Hg sequence in Table II were used to compute the values for ξ using Eq. (3), and fitted to an extrapolation formula using Eq. (8). A plot of $\cot(2\theta-2\xi)$ is shown as a long-dashed line in Fig. 1.

B. Lifetimes and line strengths

A summary of the existing lifetime data [7,18–20,23–40] for the $6s^2$-$6s6p$ transitions in the Hg isoelectronic sequence is given in Table III. The recommended lifetime values obtained from the weighted averages in Table III were converted to line strengths using wavelengths corresponding to the $J=1$ energies in Table I by use of Eq. (1). These were converted to reduced line strengths using Eqs. (4) and (5), with the empirical mixing angles θ and the values of ξ deduced from Table II. These data are presented in a plot of Z^2S_r vs $1/(Z-75)$ in Fig. 2. The solid lines represent fits to Eq. (6).

TABLE II. Ratios of radial matrix elements. Here $\Delta \equiv (R_{13}/R_{11}-1)\times 1000$.

Charge	Ion	Δ	Ion	Δ	Ion	Δ	Ion	Δ	Ion	Δ
I	Be	0.037	Mg		Zn	−1.99	Cd	−6.74	Hg	−40.2
II	B	0.113	Al	0.18	Ga	+0.16	In	−1.30	Tl	−18.2
III	C	0.212	Si	0.41	Ge	1.00	Sn	+0.35	Pb	−12.5
IV	N	0.342	P	0.61	As	1.54	Sb	1.24	Bi	−10.3
V	O	0.503	S	0.82	Se	1.97	Te	1.78	Po	−9.20
VI	F	0.682	Cl	1.04	Br	2.37	I	2.26	At	−8.64
VII	Ne	0.888	Ar	1.29	Kr	2.75	Xe	2.66	Rn	−8.27

The MCDHF calculations of the line strengths were reduced by the same procedure, using the mixing angles θ_1 and θ_3 (as defined above) for the resonance and intercombination line strengths. The loci of these values are indicated by short-dashed lines in Fig. 2.

In terms of these linearized parametrizations, the current state of knowledge of the line strengths of the $6s^2\ ^1S_1-6s6p\ ^{1,3}P_1$ transitions can be summarized very concisely by the simple formulas

$$Z^2S_r(\text{res}) = 5670[1+35.55/(Z-75)], \tag{10}$$

$$Z^2S_r(\text{int}) = 5670[1+31.57/(Z-75)], \tag{11}$$

$$\cot 2\theta = 0.3096+5.437/(Z-78), \tag{12}$$

$$R_{13}/R_{11} = 0.9931-0.0334/(Z-79)^{1.6}. \tag{13}$$

The values for the level lifetimes deduced from Eqs. (10)–(13) and the inversions of Eqs. (4), (5), and (1) are given in Table IV, together with the corresponding predictions obtained from the MCDHF calculations. The wavelength values quoted for $84 \leqslant Z \leqslant 90$ were obtained for the MCDHF calculations for the $J=1$ levels as listed in Table I.

The agreement between the semiempirical, the extrapolations, and the *ab initio* predictions provides us with good confidence in the accuracy and reliability of these results. For the measured ions Tl II, Bi III, and Bi IV, the systematic isoelectronic smoothing should generally improve the accuracy of the fitted lifetimes over those of the raw measurements. The fits also permit accurate extrapolations through the otherwise inaccessible radioactive elements.

VI. CONCLUSIONS

The approximate linearities in the measured energy level and line strength data that have been observed through their remapping as expositions of $\cot 2\theta$ and Z^2S_r plotted vs $1/(Z-C)$ (with C optimally chosen) have been verified to

TABLE III. Database of lifetime measurements (in ns). Parentheses denote quoted uncertainties.

Ion	Resonance Measurements	Wt. Avg.	Intercombination Measurements	Wt. Avg.
Hg I	1.27(10),[a] 1.31(8),[b] 1.40(8)[c] 1.34(12),[d] 1.35(5),[e] 1.36(5)[f]	1.34(3)	125(6),[g] 122(2),[h] 120(2),[i] 116(5),[j] 120(2),[k] 114(14),[l] 120.0(7),[m] 115(5),[n] 127(10),[o] 117.4(10),[p] 117(1),[q] 118(2)[r]	118.9(4)
Tl II	0.59(4)[s]	0.59(4)	39(3)[s]	39(3)
Pb III	0.380(21)[t]	0.380(21)	14.8(10),[t] 15.2(10),[u] 17.1(2)[u]	15.2(7)
Bi IV	0.243(13)[v]	0.243(13)	8.0(5),[w] 9(1),[u] 9.2(10)[u]	9.1(7)

[a]Andersen and Sørensen [23].
[b]Lurio [24].
[c]Skerbele and Lassettre [25].
[d]Abjean and Johannin [26].
[e]Pinnington *et al.* [27].
[f]Jean *et al.* [28].
[g]Benck *et al.* [29].
[h]Halstead and Reeves [30].
[i]van de Weijer and Cremers [31].
[j]Mohamed [32].
[k]Popp *et al.* [33].
[l]Nussbaum and Pipkin [34].
[m]King and Adams [35].
[n]Osherovich *et al.* [36].
[o]Andersen *et al.* [37].
[p]Dodd *et al.* [38].
[q]Deech and Baylis [39].
[r]Barrat [40].
[s]Henderson and Curtis [7].
[t]Ansbacher *et al.* [19].
[u]This work.
[v]Ansbacher *et al.* [20].
[w]Pinnington *et al.* [18].

TABLE IV. Lifetime predictions. Parentheses denote quoted or propagated uncertainties.

		Resonance				Intercombination				
Z	Ion	λ_R(Å)[a]	τ_R(ns) Expt.[c]	τ_R(ns) SE[d]	τ_R(ns) MCDHF[e]	λ_I(Å)[a]	τ_I(ns) Expt.[c]	τ_I(ns) SE[f]	τ_I(ns) MCDHF[e]	$\sin(\theta-\xi)$[b]
80	Hg I	1849.5	1.34(3)	1.346	1.086	2537.3	118.9(4)	117.9	123.5	0.1771
81	Tl II	1321.7	0.59(4)	0.602	0.543	1908.7	39(3)	36.9	36.0	0.2307
82	Pb III	1048.9	0.380(21)	0.360	0.334	1553.0	15.2(7)	16.1	16.0	0.2725
83	Bi IV	872.6	0.243(13)	0.243	0.228	1317.1	9.1(7)	8.62	8.76	0.3065
84	Po V	748.0		0.176	0.166	1146.3		5.27	5.44	0.3417
85	At VI	653.2		0.133	0.125	1019.4		3.56	3.68	0.3675
86	Rn VII	578.5		0.104	0.0979	919.9		2.57	2.65	0.3889
87	Fr VIII	517.6		0.0829	0.0781	839.2		1.94	2.00	0.4070
88	Ra IX	466.9		0.0671	0.0633	772.0		1.52	1.56	0.4223
89	Ac X	424.0		0.0550	0.0520	715.7		1.23	1.25	0.4355
90	Th XI	387.1		0.0455	0.0432	667.4		1.01	1.03	0.4469
91	Pa XII	355.0		0.0380	0.0362	625.5		0.853	0.865	0.4569
92	U XIII	326.8		0.0319	0.0305	588.7		0.728	0.736	0.4656

[a]MCDHF values from Table I for $Z \geqslant 84$.
[b]Extrapolated for $Z \geqslant 84$ using Eqs. (12) and (13).
[c]Recommended values from Table III.
[d]Semiempirical values from Eqs. (10), (12), and (13).
[e]MCDHF values from this work.
[f]Semiempirical values from Eqs. (11), (12), and (13).

persist to high Z through MCDHF calculations. These results extend the generality of a fact noted earlier for the Cd sequence [4]. Thus it can be concluded that for the Hg sequence, a few accurate lifetime measurements for ions near the neutral end can be used to make accurate extrapolative and isoelectronically smoothed predictions for the $6s^2\,{}^1S_0 - 6s6p\,{}^{1,3}P_1$ transition probability rates for all members of the sequence through $Z=92$.

ACKNOWLEDGMENTS

This work was supported by the Chemical Sciences, Geosciences, and Biosciences Division, Office of Basic Energy Sciences, Office of Science, U.S. Department of Energy, under Grant No. DE-FG02-94ER11461 (Toledo) and No. DE-FG02-97ER14761 (Vanderbilt), as well as by the Natural Sciences and Engineering Research Council of Canada.

[1] L.J. Curtis and D.G. Ellis, J. Phys. B **29**, 645 (1996).
[2] L.J. Curtis, D.G. Ellis, R. Matulioniene, and T. Brage, Phys. Scr. **56**, 240 (1997).
[3] L.J. Curtis, Phys. Scr. **63**, 104 (2001).
[4] L.J. Curtis, R. Matulioniene, D.G. Ellis, and C. Froese Fischer, Phys. Rev. A **62**, 052513 (2000).
[5] F. Parpia, C. Froese Fischer, and I.P. Grant, Comput. Phys. Commun. **94**, 249 (1996).
[6] L.J. Curtis, J. Phys. B **26**, L589 (1993).
[7] M. Henderson and L.J. Curtis, J. Phys. B **29**, L629 (1996).
[8] L.J. Curtis, Phys. Rev. A **40**, 6958 (1989).
[9] L.J. Curtis, D.G. Ellis, and I. Martinson, Phys. Rev. A **51**, 251 (1995).
[10] T. Brage, D. Leckrone, and C. Froese Fischer, Phys. Rev. A **53**, 192 (1996).
[11] D.R. Beck and Z. Cai, Phys. Rev. A **41**, 301 (1990).
[12] B.P. Das and M. Idrees, Phys. Rev. A **42**, 6900 (1990).
[13] H.-S. Chou, H.-C. Chi, and K.-N. Huang, J. Phys. B **26**, 2303 (1993).
[14] J. Migdalek and W.E. Baylis, J. Phys. B **18**, 1533 (1985).
[15] J. Migdalek and A. Bojara, J. Phys. B **21**, 2221 (1988).
[16] H.-S. Chou and K.-N. Huang, Phys. Rev. A **45**, 1403 (1992).
[17] E.H. Pinnington and W.E. Baylis, Phys. Rev. A **46**, 7325 (1992).
[18] E.H. Pinnington, W. Ansbacher, J.A. Kernahan, Z.-Q. Ge, and A.S. Inamdar, Nucl. Instrum. Methods Phys. Res. B **31**, 206 (1988).
[19] W. Ansbacher, E.H. Pinnington, and J.A. Kernahan, Can. J. Phys. **66**, 402 (1988).
[20] W. Ansbacher, E.H. Pinnington, A. Tauheed, and J.A. Kernahan, Phys. Scr. **40**, 454 (1989).
[21] L.J. Curtis, H.G. Berry, and J. Bromander, Phys. Lett. **34A**, 169 (1971).
[22] C. E. Moore, *Atomic Energy Levels*, NSRDS-NBS 35 (U.S. GPO, Washington, D.C., 1958) (reissued 1971).
[23] T. Andersen and G. Sørensen, J. Quant. Spectrosc. Radiat. Transf. **13**, 369 (1973).
[24] A. Lurio, Phys. Rev. **140**, A1505 (1965).
[25] A. Skerbele and E.N. Lassettre, J. Chem. Phys. **52**, 2708 (1972).

[26] R. Abjean and A. Johannin-Gilles, J. Quant. Spectrosc. Radiat. Transf. **16**, 369 (1976).
[27] E.H. Pinnington, W. Ansbacher, J.A. Kernahan, T. Ahmad, and Z.-Q. Ge, Can. J. Phys. **66**, 960 (1988).
[28] P. Jean, M. Martin, and D. Lecler, C. R. Acad. Sci., Ser. B **264**, 1791 (1967).
[29] E.C. Benck, J.E. Lawler, and J.T. Dakin, J. Opt. Soc. Am. B **6**, 11 (1989).
[30] J.A. Halstead and R.R. Reeves, J. Quant. Spectrosc. Radiat. Transf. **28**, 289 (1982).
[31] P. van de Weijer and R.M.M. Cremers, J. Appl. Phys. **57**, 672 (1985).
[32] K.A. Mohamed, J. Quant. Spectrosc. Radiat. Transf. **30**, 225 (1983).
[33] M. Popp, G. Schäfer, and E. Bodenstedt, Z. Phys. **240**, 71 (1970).
[34] G.H. Nussbaum and F.M. Pipkin, Phys. Rev. Lett. **19**, 1089 (1967).
[35] G.C. King and A. Adams, J. Phys. B **7**, 1712 (1974).
[36] A.L. Osherovich, E.N. Borisov, M.L. Burshteyn, and Ya.F. Verolainen, Opt. Spektrosc. **39**, 820 (1975) [Opt. Spectrosc. **39**, 466 (1975)].
[37] T. Andersen, K.A. Jessen, and G. Sørensen, Nucl. Instrum. Methods **90**, 35 (1971).
[38] J.N. Dodd, W.J. Sandle, and O.M. Williams, J. Phys. B **3**, 256 (1970).
[39] J.S. Deech and W.E. Baylis, Can. J. Phys. **49**, 90 (1971).
[40] J.P. Barrat, J. Phys. Radium **20**, 657 (1959).